Free oscillations in an elliptic membrane

J. Gutiérrez-Vega and S. Chávez-Cerda
Grupo de Fotónica y Física Óptica, Instituto Nacional de Astrofísica Óptica y Electrónica
Apartado postal 51 y 216, 72000 Puebla, Pue., Mexico

Ramón Rodríguez-Dagnino
Centro de Electrónica y Telecomunicaciones, Instituto Tecnológico y de Estudios Superiores de Monterrey
Garza Sada 2501, Col. Tecnológico, Monterrey, N.L., Mexico

Recibido el 25 de mayo de 1999; aceptado el 12 de julio de 1999

An study of the classical problem of the free oscillations in an elliptic membrane is presented. The oscillating modes are characterized by Mathieu and modified Mathieu functions. We emphasize the differences between the circular and elliptic membranes. A relation to obtain the number of nodal points of a particular oscillating mode is presented. We have taken advantage of the modern computational tools to illustrate several vibrations modes patterns which appear in an elliptic membrane.

Keywords: Membrane; Mathieu; elliptic coordinates

Se presenta un estudio del problema clásico de las oscilaciones libres en una membrana elíptica. Los modos de oscilación se pueden caracterizar por medio de las funciones ordinarias y modificadas de Mathieu. Se enfatiza en las diferencias entre la membrana circular y la elíptica. Se presenta una relación para calcular el número de puntos nodales de un modo de oscilación en particular. Hemos tomado ventaja de las modernas técnicas computacionales para mostrar varios patrones típicos de los modos de oscilación que aparecen en la membrana elíptica.

Descriptores: Membrana; Mathieu; coordenadas elípticas

PACS: 02.30.-f; 02.30.Jr

1. Introduction

The problem of finding the natural vibrational modes of a membrane is a classical problem in mathematical-physics when studying the wave equation in two dimensions. The rectangular and circular geometries are very well studied in basic texts [1–3]. In fact, the fundamental solution of the circular membrane dates back to 1764 by L. Euler who established that the vibration modes can be expressed as a linear combination of Bessel functions. However, the elliptic membrane has interesting phenomena which deserve further study. This elliptic geometry was originally studied by E. Mathieu in 1868 [4], he introduced the special functions, now called them after him. The vibrational modes of the elliptic membrane can be expressed as a linear combination of Mathieu functions. A brief description of this problem only appears in very specialized books [5]. More recently, L. Ruby [6] barely mentions the problem of the vibrations in an elliptic drum as an application of Mathieu equation. A very simple experimental setup to study elliptical modes could be for instance, the water surface of an elliptical tub.

On the other hand, the theory of Mathieu functions has evolved in its own, so our purpose in this paper is to present an extensive analysis of the classical problem of free oscillations in an elliptic membrane by using a more elaborated theory of the Mathieu functions and by taking advantage of modern computational tools. With these, we present a graphical illustration of several vibrational mode patterns in two and three dimensions. We analyze the situations of different ellipticities in the membrane boundary.

The paper is organized as follows. In Sect. 2 we introduce the definition of elliptic coordinates and with them, we write the 2D wave equation in these coordinates. The solution of the wave equation is presented in Sect. 3. Different boundary conditions are stated in Sect. 4, and numerical results are given in Sect. 5. Finally, in the Conclusions we point out some interesting differences with respect to the circular geometry.

1.1. Preliminaries

We understand for an elliptic membrane a thin sheet of elastic material in a state of uniform and constant tension. To make our analysis, we will consider the ellipse centered in the xy-plane with its semi-major axis a and semi-minor axis b, as it is shown in the Fig. 1. The foci of the ellipse, in this reference frame, are located at $(x = \pm f, y = 0)$, where the foci $\pm f$ are given by $f^2 = a^2 - b^2$.

Let σ be the superficial mass density of the membrane and F the uniform tension per unit length in each point of the membrane. Let us consider that the membrane has a small displacement with respect to the plane $z = 0$ in such a manner that we can assume that each point moves parallel to the z-axis with simple harmonic motion.

Let $\varphi(\vec{r}, t)$ be the displacement as a function of time of a point of the membrane located at $\vec{r}$, then the *wave equation*

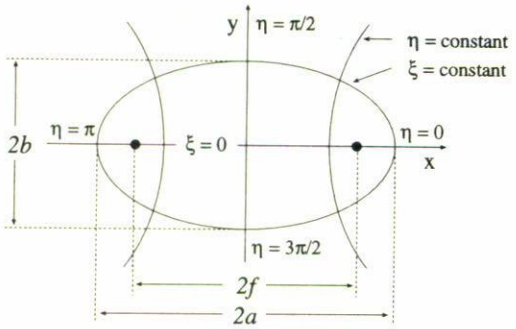

FIGURE 1. Elliptic coordinates.

associated to φ is given by

$$\nabla^2\varphi = \frac{1}{v^2}\frac{\partial^2\varphi}{\partial t^2}, \tag{1}$$

where

$$\frac{1}{v^2} = \frac{\sigma}{F}. \tag{2}$$

A detailed treatment of the physical derivation of the wave equation in membranes can be found in Simmons [1]. Observe that to this point there is no difference of the wave equation with respect to the coordinate system. In the next section we will define the elliptic coordinates and with them the Laplacian operator in these coordinates.

2. Wave equation in elliptic coordinates

The elliptic coordinates are defined according to the transformation $x + iy = f\cosh(\xi + i\eta)$. Now, by equating the real and the imaginary parts of each side we obtain

$$x = f\cosh\xi\cos\eta; \quad y = f\sinh\xi\sin\eta, \quad z = z \tag{3}$$

that satisfy

$$\frac{x^2}{f^2\cosh^2\xi} + \frac{y^2}{f^2\sinh^2\xi} = \cos^2\eta + \sin^2\eta = 1, \tag{4}$$

$$\frac{x^2}{f^2\cos^2\eta} - \frac{y^2}{f^2\sin^2\eta} = \cosh^2\xi - \sinh^2\xi = 1. \tag{5}$$

Equation (4) represents a family of confocal ellipses with semi-major axis $a = f\cosh\xi$ and semi-minor axis $b = f\sinh\xi$. Similarly, Eq. (5) represents a family of confocal hyperbolas with the same foci as the ellipses (Fig. 1). The two families of conics intersect orthogonally and each intersection corresponds to a point in the xy-plane defined by Eqs. (3).

The ranges of coordinates are given by

$$0 \le \xi < \infty, \qquad 0 \le \eta < 2\pi, \qquad -\infty < z < \infty.$$

In order to obtain the wave equation in elliptic coordinates, the Laplacian operator expressed in general-coordinates is defined as follows:

$$\nabla^2 = \sum_{i=1}^{3}\frac{1}{h_i^2}\frac{\partial^2}{\partial q_i^2}, \tag{6}$$

where $q_1 = \xi$, $q_2 = \eta$, $q_3 = z$ and the scale factors are given by

$$h_1 = h_2 = f\sqrt{\frac{1}{2}(\cosh 2\xi - \cos 2\eta)}, \qquad h_3 = 1. \tag{7}$$

By combining Eqs. (1), (6) and (7) and the since the displacement function φ depends only on the transverse coordinates, $(i.e. \partial^2\varphi/\partial z^2 = 0)$, we obtain the 2D-wave equation

$$\frac{2}{f^2(\cosh 2\xi - \cos 2\eta)}\left(\frac{\partial^2\varphi}{\partial\xi^2} + \frac{\partial^2\varphi}{\partial\eta^2}\right) = \frac{1}{v^2}\frac{\partial^2\varphi}{\partial t^2}, \tag{8}$$

where $\varphi = \varphi(\xi, \eta, t)$.

3. The solution of the wave equation

We apply the separation of variables method to solve the wave equation (8). Let us suppose that

$$\varphi(\xi, \eta, t) = R(\xi)\Theta(\eta)T(t), \tag{9}$$

where we can set

$$U(\xi, \eta) = R(\xi)\Theta(\eta) \tag{10}$$

as the spatial solution of the wave equation. In order to separate the variables, we substitute Eq. (9) in (8), and we obtain the three following differential equations:

$$T''(t) + k^2v^2T = 0, \tag{11}$$

$$R''(\xi) - (\alpha - 2q\cosh 2\xi)\,R(\xi) = 0, \tag{12}$$

$$\Theta''(\eta) + (\alpha - 2q\cos 2\eta)\,\Theta(\eta) = 0, \tag{13}$$

where $-k^2$ and α are the constants of separation and q is a parameter given by

$$q = \frac{k^2f^2}{4} = \frac{\omega^2f^2\sigma}{4F}. \tag{14}$$

As we will see later, the negative sign of k^2 is chosen to have oscillatory solutions in time, whereas exponential related solutions are obtained with the positive sign.

Equations (12) and (13) are known as *Modified Mathieu Equation* (MME) and *Ordinary Mathieu Equation* (OME), respectively. Their solutions are known as *Modified Mathieu Functions* (MMF) and *Ordinary Mathieu Functions* (OMF), respectively.

The spatial solution $U(\xi, \eta)$ is the product of solutions of Eqs. (12) and (13) for *the same value of* α *and* q.

If in Eq. (11) we set $\omega = kv$ we obtain the *harmonic equation* $T'' + \omega^2T = 0$ whose solutions are

$$T(t) = A\cos\omega t + B\sin\omega t, \tag{15}$$

where A and B are constants that are determined by the initial conditions of the problem.

3.1. Solution of the Mathieu Equations

We will require that the OME (13) has periodic solutions with period 2π. The values of α that satisfy this condition are known as *characteristic values* and they generate an infinite set of real values that have the property $\alpha_0 < \alpha_1 < \alpha_2 < \cdots$. When the solutions are symmetrical with respect to $\eta = 0$, we express the characteristic numbers as $\alpha_r(q) : (r = 0, 1, 2, \cdots)$, and for the case of anti-symmetric solutions we have $\beta_r(q) : (r = 1, 2, 3, \cdots)$.

The periodic solutions for Eq. (13) can be obtained by using the Fourier series [5, 7].

$$\Theta(q, \eta) = \sum_{k=0}^{\infty} [A_k(q) \cos k\eta + B_{k+1}(q) \sin(k+1)\eta]. \quad (16)$$

This solution is usually separated into two parts as follows

$$ce_r(q, \eta) = \sum_{k=0}^{\infty} A_k \cos k\eta$$

and

$$se_{r+1}(q, \eta) = \sum_{k=1}^{\infty} B_k \sin k\eta,$$

where $ce_r(q, \eta)$ and $se_{r+1}(q, \eta)$ are known as the *even Mathieu function* of r-order and the *odd Mathieu function* of $(r+1)$-order, respectively.

If we substitute Eq. (16) in (13) we can obtain the following recurrence relations for the Fourier coefficients for a particular characteristic value α_r or β_r. We have different relations for r even or odd, then we set r equal to $2n$ or $2n+1$ accordingly, where $n \geq 0$.

$ce_{2n} : (\alpha = \alpha_{2n}); \quad (k \geq 2)$

$$\alpha A_0 = qA_2, \quad (17a)$$

$$(\alpha - 4)A_2 = q(2A_0 + A_4), \quad (17b)$$

$$\left[\alpha - (2k)^2\right] A_{2k} = q(A_{2k-2} + A_{2k+2}). \quad (17c)$$

$ce_{2n+1} : (\alpha = \alpha_{2n+1}); \quad (k \geq 1)$

$$(\alpha - 1)A_1 = q(A_1 + A_3), \quad (18a)$$

$$\left[\alpha - (2k+1)^2\right] A_{2k+1} = q(A_{2k-1} + A_{2k+3}). \quad (18b)$$

$se_{2n+2} : (\beta = \beta_{2n+2}); \quad (k \geq 2)$

$$(\beta - 4)B_2 = qB_4, \quad (19a)$$

$$\left[\beta - (2k)^2\right] B_{2k} = q(B_{2k-2} + B_{2k+2}). \quad (19b)$$

$se_{2n+1} : (\beta = \beta_{2n+1}); \quad (k \geq 1)$

$$(\beta - 1)B_1 = q(B_3 - B_1), \quad (20a)$$

$$\left[\beta - (2k+1)^2\right] B_{2k+1} = q(B_{2k-1} + B_{2k+3}). \quad (20b)$$

In order to have periodic solutions for the above recurrence relations, the characteristic values must satisfy the following continued fractions [7]

$$V_0 = \frac{2}{V_{2-}} \frac{1}{V_{4-}} \frac{1}{V_{6-}} \cdots ; (\text{Roots} = \alpha_{2n}) \quad (21)$$

$$V_1 - 1 = \frac{1}{V_{3-}} \frac{1}{V_{5-}} \frac{1}{V_{7-}} \cdots ; (\text{Roots} = \alpha_{2n+1}) \quad (22)$$

$$V_2 = \frac{1}{V_{4-}} \frac{1}{V_{6-}} \frac{1}{V_{8-}} \cdots ; (\text{Roots} = \beta_{2n+2}) \quad (23)$$

$$V_1 + 1 = \frac{1}{V_{3-}} \frac{1}{V_{5-}} \frac{1}{V_{7-}} \cdots ; (\text{Roots} = \beta_{2n+1}), \quad (24)$$

where

$$V_j = \frac{(\alpha - j^2)}{q}; \quad (j \geq 0). \quad (25)$$

The continued fractions (21)–(24) are equations for α or β. The roots are in fact the characteristic values α_r and β_r of the Mathieu functions.

Once the characteristic values are calculated by solving Eqs. (21)–(24), the recurrence relations (17a)–(20b) should be applied to obtain the Fourier coefficients of the series (16). The OMF are expressed finally as follows

$$ce_{2n}(q, \eta) = \sum_{k=0}^{\infty} A_{2k}(q) \cos 2k\eta, \quad (26)$$

$$ce_{2n+1}(q, \eta) = \sum_{k=0}^{\infty} A_{2k+1}(q) \cos(2k+1)\eta, \quad (27)$$

$$se_{2n+2}(q, \eta) = \sum_{k=0}^{\infty} B_{2k+2}(q) \sin(2k+2)\eta, \quad (28)$$

$$se_{2n+1}(q, \eta) = \sum_{k=0}^{\infty} B_{2k+1}(q) \sin(2k+1)\eta. \quad (29)$$

As a consequence of the orthogonality property of the sine and cosine series, the OMF ce_r and se_{r+1} are orthogonal functions:

$$\int_0^{2\pi} ce_m(q, z) ce_p(q, z) dz = \int_0^{2\pi} se_m(q, z) se_p(q, z) dz = \begin{cases} \pi & \text{if } m = p \\ 0 & \text{if } m \neq p. \end{cases} \quad (30)$$

By substituting Eqs. (26)–(29) in (30) we can obtain the following normalization relations:

$$2A_0^2 + \sum_{k=1}^{\infty} (A_{2k})^2 = \sum_{k=0}^{\infty} (A_{2k+1})^2 = \sum_{k=0}^{\infty} (B_{2k+2})^2 = \sum_{k=0}^{\infty} (B_{2k+1})^2 = 1. \quad (31)$$

The MME (12) is obtained from the OME (13) by setting the change of variable $\eta = i\xi$. Therefore we can apply

this change of variable to OMF Eqs. (26)–(29) to obtain the following MMFs.

$$Ce_{2n}(q,\xi) = \sum_{k=0}^{\infty} A_{2k}(q)\cosh 2k\xi, \tag{32}$$

$$Ce_{2n+1}(q,\xi) = \sum_{k=0}^{\infty} A_{2k+1}(q)\cosh(2k+1)\xi, \tag{33}$$

$$Se_{2n+2}(q,\xi) = \sum_{k=0}^{\infty} B_{2k+2}(q)\sinh(2k+2)\xi, \tag{34}$$

$$Se_{2n+1}(q,\xi) = \sum_{k=0}^{\infty} B_{2k+1}(q)\sinh(2k+1)\xi, \tag{35}$$

where $Ce_r(q,\xi)$ is the *even modified Mathieu function* of r-order and $Se_{r+1}(q,\xi)$ is the *odd modified Mathieu function* of $(r+1)$-order.

The MMF Eqs. (32)–(35) can also be expressed by using Bessel functions series [5]. In Appendix A we show the Bessel-series representation for MMF.

3.2. General solution of the wave equation

The spatial solution of the wave-equation is given by

$$U(\xi,\eta) = \sum_{r=0}^{\infty} U_r(\xi,\eta) = \sum_{r=0}^{\infty} R_r(\xi)\Theta_r(\eta)$$
$$= \sum_{r=0}^{\infty} \begin{cases} Ce_r(q,\xi)ce_r(q,\eta) \\ Se_{r+1}(q,\xi)se_{r+1}(q,\eta). \end{cases} \tag{36}$$

Combining the time-solution Eq. (15) with the spatial-solution Eq. (36) we obtain the general solution of the wave-equation in elliptic coordinates

$$\varphi(\xi,\eta,t) = \sum_{r=0}^{\infty} \begin{Bmatrix} Ce_r(q,\xi)ce_r(q,\eta) \\ Se_{r+1}(q,\xi)se_{r+1}(q,\eta) \end{Bmatrix} \times (A_r\cos\omega t + B_r\sin\omega t), \tag{37}$$

where q is given by Eq. (14).

4. Boundary conditions and notation

Since $\varphi(\xi,\eta,t)$ should be single valued then the first boundary condition is given by

$$\varphi(\xi,\eta,t) = \varphi(\xi,\eta+2\pi,t), \tag{38}$$

and the Mathieu functions $ce_r(q,\eta)$ and $se_{r+1}(q,\eta)$ result appropriate in this case. The elliptic boundary of the membrane is given by $\xi = \xi_0 =$ constant, and the eccentricity e of the ellipse is defined as

$$e = \frac{f}{a} = \frac{1}{\cosh\xi_0}. \tag{39}$$

On the elliptic boundary $[\xi = \xi_0]$ the membrane is fixed, therefore $\varphi(\xi_0,\eta,t) = 0$ for any η and t. This condition is satisfied when

$$R_r(\xi_0) = \begin{cases} Ce_r(q,\xi_0) \\ Se_{r+1}(q,\xi_0) \end{cases} = 0. \tag{40}$$

MMF are decreasing-oscillatory non-periodic functions similar to the Bessel functions. Therefore, if we choose a certain harmonic r we have an infinite set of possible values of q that satisfy (40).

Let $q_{r,m}$ the m-th zero of MMF of r-order. According to Eq. (14) for each $q_{r,m}$ there exist a corresponding frequency $\omega_{r,m}$, and by solving Eq. (14) for ω we can obtain

$$\omega_{r,m} = \sqrt{\frac{4q_{r,m}}{f^2}\frac{F}{\sigma}}. \tag{41}$$

For the sake of clarity, we will associate the term *harmonic* to r $(r \geq 0)$ and the term *mode* to m $(m \geq 1)$. In this manner, the function $\varphi_{03}(\xi,\eta,t)$ corresponds to the third mode $(m=3)$ of the first harmonic $(r=0)$.

We will use the subindex e and o to refer to even and odd modes respectively. Excepting the first harmonics $r=0$, all modes can be even or odd.

By using this notation, the general solution for the membrane, with the previous boundary conditions, can be expressed in the following form:

Even modes

$${}_e\varphi(\xi,\eta,t) = \sum_{r=0}^{\infty}\sum_{m=1}^{\infty} {}_e\varphi_{r,m}(\xi,\eta,t) = \sum_{r=0}^{\infty}\sum_{m=1}^{\infty} C_{r,m}Ce_r({}_eq_{r,m},\xi)ce_r({}_eq_{r,m},\eta)$$
$$\times \left[{}_eA_{r,m}\cos({}_e\omega_{r,m}t) + {}_e B_{r,m}\sin({}_e\omega_{r,m}t)\right], \tag{42}$$

where ${}_eA_{r,m}$, ${}_eB_{r,m}$ and $C_{r,m}$ are constants determined by the initial conditions.

Odd modes

$${}_o\varphi(\xi,\eta,t) = \sum_{r=1}^{\infty}\sum_{m=1}^{\infty} {}_o\varphi_{r,m}(\xi,\eta,t) = \sum_{r=1}^{\infty}\sum_{m=1}^{\infty} S_{r,m}Se_r({}_oq_{r,m},\xi)se_r({}_oq_{r,m},\eta)$$
$$\times \left[{}_oA_{r,m}\cos({}_o\omega_{r,m}t) + {}_oB_{r,m}\sin({}_o\omega_{r,m}t)\right]. \tag{43}$$

The complete solution to the problem of the membrane is the superposition of even and odd modes

$$\varphi(\xi,\eta,t) = {}_e\varphi(\xi,\eta,t) + {}_o\varphi(\xi,\eta,t) \tag{44}$$

4.1. Transition to circular membrane

Now, we will see how the circular membrane can be obtained as a particular case of the elliptical one. If we assume that the ellipse tends to a circle of radius a, then from Fig. 1 we appreciate that $b \to a$, and from Eq. (39) we notice that $f \to 0$, $e \to 0$ and $\xi_0 \to \infty$. Similarly, when $f \to 0$, we obtain from Eq. (14) that $q \to 0$ as well.

The Mathieu equations Eqs. (12) and (13) are simplified accordingly. In particular when $q = 0$ the OME (13) becomes the harmonic equation $\Theta''(\eta) + \alpha\Theta(\eta) = 0$, whose periodic solutions are given by $\Theta(\eta) = A\cos\sqrt{\alpha}\eta + B\sin\sqrt{\alpha}\eta$, where A and B are arbitrary constants. To ensure periodic solutions, with period 2π, we need to establish $\sqrt{\alpha} = r = 0, 1, 2, \cdots$. Hence the characteristic values, say α_r, are

$$\alpha_r = r^2 = 0, 1, 4, 9, \cdots \tag{45}$$

In the same manner, when $q = 0$, the recurrence relations Eqs. (17a)–(20b) reduce to

$$\left(\alpha - k^2\right) A_k = 0; \qquad k = 0, 1, 2, \cdots \tag{46}$$

and by Eq. (45) the only value of k that satisfies Eq. (46) is $k = r$. Hence all Fourier coefficients A_k (or B_k) in OMF Eqs. (26)–(29) with $k \neq r$ must vanish. Additionally, to be consistent with the normalization (31) we define

$$A_k, B_k = \begin{cases} 0 & \text{if } k \neq r \\ 1 & \text{if } k = r. \end{cases} \tag{47}$$

The OMF Eqs. (26)–(29) can be simplified by using the result (47) and the fact that $e \to 0$ (*i.e.* $q \to 0$)

$$ce_r(q,\eta) \to \cos r\eta \quad \text{and} \quad se_r(q,\eta) \to \sin r\eta.$$

The implications of setting $q \to 0$ in the MME (12) are not quite straighforward, this is due to Eq. (39) where $\xi \to \infty$ and the term

$$2q\cosh 2\xi = 2q\left(\frac{e^{2\xi} + e^{-2\xi}}{2}\right) \to qe^{2\xi}.$$

By using this results and Eq. (45) the MMEs (12) degenerates to

$$R''(\xi) + \left(qe^{2\xi} - r^2\right) R(\xi) = 0. \tag{48}$$

Now by defining the circular radius $\rho = (f/2)e^{\xi}$ and using the first equality in Eq. (14), then the Eq. (48) can be transformed into the Bessel equation

$$R''(\rho) + \frac{1}{\rho}R'(\rho) + \left(k^2 - \frac{r^2}{\rho^2}\right) R(\rho) = 0,$$

whose solutions are the Bessel functions $R(\rho) = J_r(k\rho)$. Therefore as $e \to 0$,

$$Ce_r(q,\xi) \to P\, J_r(k\rho) \quad \text{and} \quad Se_r(q,\xi) \to S\, J_r(k\rho),$$

where P and S are scaling factors to maintain normalization.

The boundary condition is satisfied when $J_r(ka) = 0$. Using Eq. (2) and $\omega = vk$ the characteristic vibration frequencies can be obtained by

$$\omega_{r,m} = \frac{q_{r,m}}{a}\sqrt{\frac{F}{\sigma}} \tag{49}$$

where $q_{r,m}$ is the m-th zero of the J_r Bessel function and a is the membrane radius.

Finally, the spatial solution in the elliptic membrane Eq. (36) degenerates to a well-known expression for the circular membrane

$$\begin{aligned} U(\rho,\eta) &= \sum_{r=0}^{\infty}\sum_{m=1}^{\infty} U_{r,m}(\rho,\eta) \\ &= \sum_{r=0}^{\infty}\sum_{m=1}^{\infty} [C_{r,m}J_r(k_{r,m},\rho)\cos r\eta] \\ &\qquad + [S_{r,m}J_r(k_{r,m},\rho)\sin r\eta] \end{aligned} \tag{50}$$

where $k_{r,m} = q_{r,m}/a$ and $C_{r,m}$ and $S_{r,m}$ are constants to be determined from the initial shape of the membrane.

5. Numerical results

In this section we present tables of *characteristic vibrational frequencies* for membranes with different eccentricities including the circular membrane. We show plots of the Mathieu functions and mode-patterns for the first, second and third harmonic respectively and we analyze the superposition of the even and odd modes. In the next calculations, without loss of generality, we will select the tension and density of the membrane such that

$$\sqrt{F/\sigma} = 1. \tag{51}$$

5.1. Tables of characteristic vibration frequencies

In order to obtain reference values of characteristic frequencies, we first consider a circular membrane with radius a=5 cm. The general solution is given by Eq. (50) and the characteristic frequencies are calculated by using Eq. (49) with (51). In Table I we show the frequencies for the first two modes of the first three harmonics.

In the following example we consider the elliptic case. Now, the frequencies are calculated by using Eq. (41). As above, in Table II we show the frequencies for the first two modes of the first three harmonics. The axes still have similar values, however it is enough to show that each circular mode splits into an even mode and an odd mode. From Table II we can see that the even modes have lower frequencies than odd

TABLE I. Characteristic frequencies for the circular membrane: $a = 5$ cm, $e = 0$.

Order	Mode m	
r	1	2
0	48.097	110.402
1	76.634	140.312
2	102.712	168.345

TABLE II. Characteristic frequencies for the elliptic membrane: $a = 5$ cm, $b = 4.9$ cm, $e = 0.2$, $\xi_0 = 2.298$.

Order	Even modes		Odd modes		${}_o\omega_{r,m}/{}_e\omega_{r,m}$	
r	1	2	1	2	1	2
0	48.590	111.603	–	–	–	–
1	77.027	141.065	77.809	142.49	1.0102	1.0101
2	103.690	169.802	103.764	170.103	1.0007	1.0018

TABLE III. Characteristic frequencies for the elliptic membrane: $a = 5$ cm, $b = 3$ cm, $e = 0.8$, $\xi_0 = 0.693$

Order	Even modes		Odd modes		${}_o\omega_{r,m}/{}_e\omega_{r,m}$	
r	1	2	1	2	1	2
0	65.865	168.496	-	-	-	-
1	91.546	191.229	116.513	220.672	1.273	1.154
2	118.880	214.983	139.813	243.083	1.176	1.131

TABLE IV. Characteristic frequencies for the elliptic membrane: $a = 5$ cm, $b = 2$ cm, $e = 0.92$, $\xi_0 = 0.4236$

Order	Even modes		Odd modes		${}_o\omega_{r,m}/{}_e\omega_{r,m}$	
r	1	2	1	2	1	2
0	90.514	246.363	-	-	-	-
1	114.080	267.814	168.078	324.782	1.473	1.213
2	139.416	290.020	189.992	346.009	1.363	1.193

modes (${}_e\omega_{r,m} < {}_o\omega_{r,m}$). The reason is that to even modes vibrate along the largest axis of the ellipse. In this case, the frequencies in even and odd modes are still very similar to the circular case.

When we increase the eccentricity to 0.8 and 0.92 (Tables III and IV) by maintaining the longitude of major axis constant, we can see that the frequencies increase notoriously. We should also notice the increment in ratios ${}_o\omega_{r,m}/{}_e\omega_{r,m}$ with respect to the case shown in the Table II.

Finally in Table V we show the case of an membrane with a very high eccentricity, namely $e = 0.99$. Here we can observe a larger difference between the even and odd modes frequencies. Now the frequency of the lowest mode ${}_e\varphi_{01}$ is 430% greater than the circular membrane.

TABLE V. Characteristic frequencies for the elliptic membrane: $a = 5$ cm, $b = 0.8$ cm, $e = 0.99$, $\xi_0 = 0.16$

Order	Even mode	Odd mode	${}_o\omega_{r,m}/{}_e\omega_{r,m}$
r	1	1	1
0	206.955	–	–
1	228.125	403.009	1.766
2	250.204	423.619	1.693

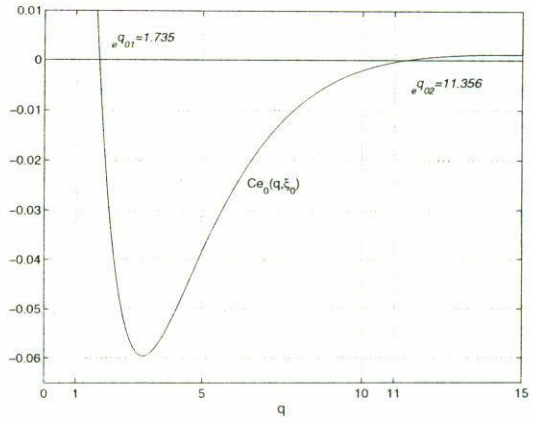

FIGURE 2. Plot of Mathieu function $Ce_0(q, \xi_0)$ as a function of q and $\xi_0 = 0.693$.

5.2. Fundamental harmonics

The fundamental harmonics correspond to $r = 0$ and they are present only in even modes. By using Eq. (42) we can obtain the equations corresponding to the first two modes. We should set ${}_eB_{01} = {}_eB_{02} = 0$ and ${}_eA_{01} = {}_eA_{02} = 1$, and the modes are given by

$$
\begin{aligned}
{}_e\varphi_{01}(\xi,\eta,t) &= {}_eU_{01}(\xi,\eta)T_{01}(t) \\
&= Ce_0({}_eq_{01},\xi)\; ce_0({}_eq_{01},\eta)\cos({}_e\omega_{01}t) \qquad (52)\\
{}_e\varphi_{02}(\xi,\eta,t) &= {}_eU_{02}(\xi,\eta)T_{02}(t) \\
&= Ce_0({}_eq_{02},\xi)\; ce_0({}_eq_{02},\eta)\cos({}_e\omega_{02}\,t)\,. \qquad (53)
\end{aligned}
$$

To show a typical case we consider an ellipse with $e = 0.8$ and the parameters from Table III. The boundary condition Eq. (40) can be expressed as $Ce_0({}_eq_{0,m},\xi_0) = 0$. The plot of $Ce_0(q,\xi_0)$ as a function of q is shown in Fig. 2. We are only showing the first two zeros of the function and they occur at ${}_eq_{01} = 1.735$ and ${}_eq_{02} = 11.356$. By using Eq. (41) the corresponding frequencies are ${}_e\omega_{01} = 65.866$ rad/s and ${}_e\omega_{02} = 168.496$ rad/s.

In Fig. 3 we show the plots of Mathieu functions $Ce_0({}_eq_{01},\xi)$, $Ce_0({}_eq_{02},\xi)$, $ce_0({}_eq_{01},\eta)$ and $ce_0({}_eq_{02},\eta)$. We can see that $ce_0({}_eq_{01},\eta)$ and $ce_0({}_eq_{02},\eta)$ have period π and are never negative. This property is a general characteristic of the zero-order Mathieu functions $ce_0(q,\eta)$. In the same

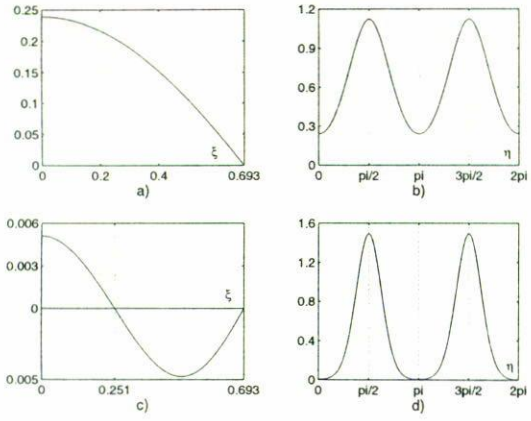

FIGURE 3. Plots of even Mathieu functions corresponding to first two modes of the first harmonic: *a)* $Ce_0({}_eq_{01},\xi)$; *b)* $ce_0({}_eq_{01},\eta)$; *c)* $Ce_0({}_eq_{02},\xi)$ and *d)* $ce_0({}_eq_{02},\eta)$. In this case there exists only even modes and OMF are always positive.

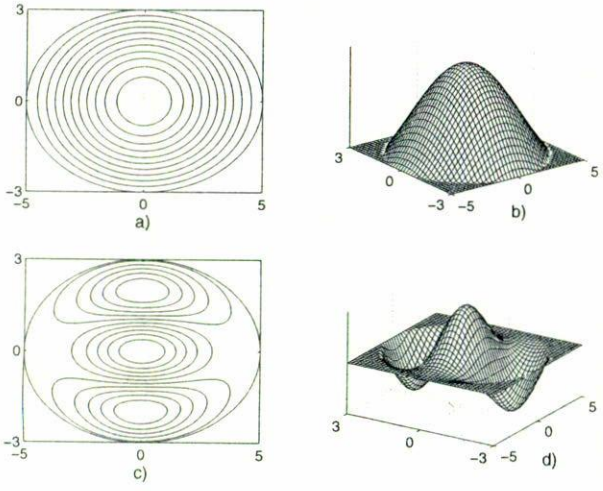

FIGURE 4. Contour and 3-D plots of *a,b)* the lowest spatial mode ${}_eU_{01}(\xi,\eta)$; and *c,d)* the second mode ${}_eU_{02}(\xi,\eta)$. The lowest mode is the only mode that never have nodal lines. On the contrary, the second mode presents a elliptic nodal line. Evidently, the number of elliptic nodal lines increases as modes increase.

manner, we can appreciate that $Ce_0({}_eq_{01},\xi)$ is positive for $\xi < \xi_0$. Therefore, by using Eq. (52), the spatial mode ${}_eU_{01}$ is always positive and we can conclude that it does not present nodal-lines. In Fig. 3c we can notice that $Ce_0({}_eq_{02},\xi)$ has a zero at $\xi = 0.251$, hence the second spatial mode ${}_eU_{02}$ presents an elliptic nodal-line. Contour and 3-D plots of the spatial modes ${}_eU_{01}(\xi,\eta)$ and ${}_eU_{02}(\xi,\eta)$ are shown in Fig. 4.

5.3. Second harmonics

The second harmonics correspond to $r = 1$ and now they are present in even and odd modes.

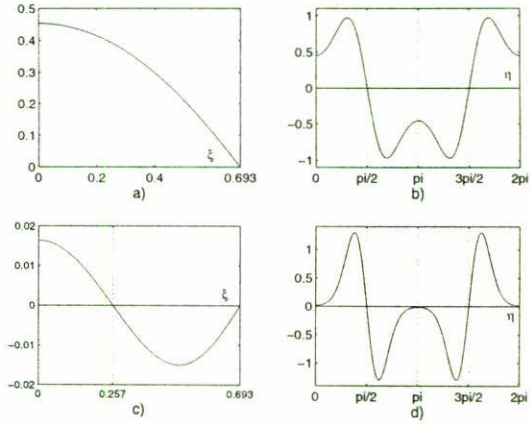

FIGURE 5. Plots of even Mathieu functions corresponding to second harmonic: a) $Ce_1({}_eq_{11},\xi)$; b) $ce_1({}_eq_{11},\eta)$; c) $Ce_1({}_eq_{12},\xi)$; d) $ce_1({}_eq_{12},\eta)$. In this case the OMFs have period 2π and present nodal lines at $\eta = \pi/2$ and $\eta = 3\pi/2$.

5.3.1. *Even modes*

The equations for the first two even spatial modes of the second harmonic are given by

$$ {}_eU_{11}(\xi,\eta) = Ce_{11}({}_eq_{11},\xi)ce_{12}({}_eq_{11},\eta), $$

$$ {}_eU_{12}(\xi,\eta) = Ce_{12}({}_eq_{12},\xi)ce_{12}({}_eq_{12},\eta), $$

where ${}_eq_{11} = 3.352$ and ${}_eq_{12} = 14.627$.

In Fig. 5 we show the plots of *one*-order-even Mathieu functions $Ce_1({}_eq_{11},\xi)$, $Ce_1({}_eq_{12},\xi)$, $ce_1({}_eq_{11},\eta)$ and $ce_1({}_eq_{12},\eta)$. We can appreciate that the main differences with respect to the zero-order plots (Fig. 3) are that ordinary functions $ce_1({}_eq_{11},\eta)$ and $ce_1({}_eq_{12},\eta)$ have period 2π and that they present two zeros at $\eta = \pi/2$ and $\eta = 3\pi/2$. Hence the even modes of the second harmonics present a straight nodal-line at y-axis, as it is shown in Fig. 7. In addition to this, we can notice in Fig. 7b that ${}_eU_{12}(\xi,\eta)$ presents an elliptic nodal-line at $\xi = 0.257$ corresponding to the first zero of $Ce_1({}_eq_{12},\xi)$ in Fig. 5c.

5.3.2. *Odd Modes*

The equations for the first two odd spatial modes of the second harmonic are given by

$$ {}_oU_{11}(\xi,\eta) = Se_{11}({}_oq_{11},\xi)se_{12}({}_oq_{11},\eta), $$

$$ {}_oU_{12}(\xi,\eta) = Se_{12}({}_oq_{12},\xi)se_{12}({}_oq_{12},\eta), $$

where ${}_oq_{11} = 5.430$ and ${}_oq_{12} = 19.478$.

We can observe in Fig. 6 that $Se_1({}_oq_{11},\xi)$ and $Se_1({}_oq_{12},\xi)$ present a zero at $\xi = 0$ and that $se_1({}_oq_{11},\eta)$ and $se_1({}_oq_{12},\eta)$ present two zeros at $\eta = 0$ and $\eta = \pi$. Therefore the odd modes present a straight nodal-line at x-axis. This nodal-line is shown in Figs. 7c and 7d. As in the even case, for the second mode we can also appreciate an elliptic nodal-line corresponding to $\xi = 0.369$.

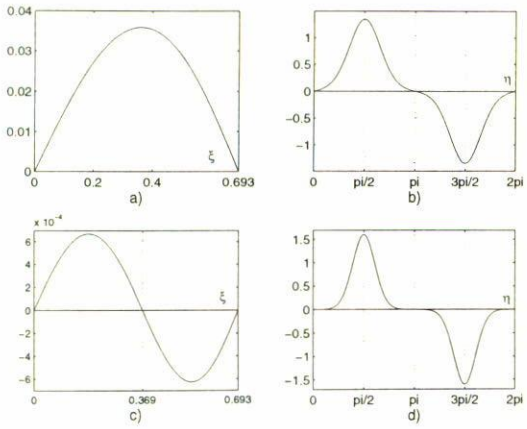

FIGURE 6. Plots of odd Mathieu functions: a)$Se_1({}_oq_{11},\xi)$; b) $se_1({}_oq_{11},\eta)$ c) $Se_1({}_oq_{12},\xi)$; d) $se_1({}_oq_{12},\eta)$. As similar at even modes, in this case the OMFs presents two nodal lines as well, but now, at $\eta = 0$ and $\eta = \pi$.

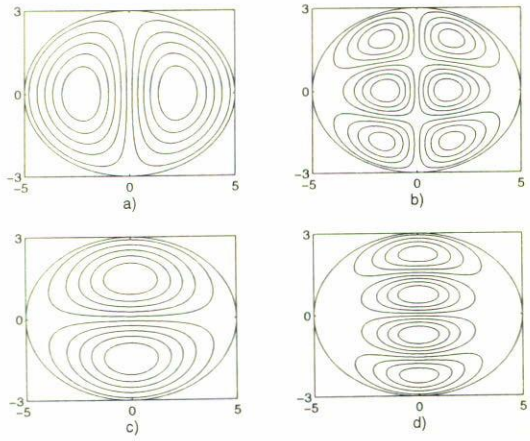

FIGURE 7. Contour plots of second harmonics a)${}_eU_{11}(\xi,\eta)$; b) ${}_eU_{12}(\xi,\eta)$; c) ${}_oU_{11}(\xi,\eta)$; d) ${}_oU_{12}(\xi,\eta)$. The even modes present a vertical straight nodal line corresponding at $\eta = \pi/2$ and $\eta = 3\pi/2$, whereas the odd modes present a horizontal straight nodal line.

5.4. Third harmonics

We show the mode-patterns of ${}_{e,o}U_{21}$ and ${}_{e,o}U_{22}$ in Fig. 8 to illustrate an example of modes which present two angular nodal-lines: *1)* the even modes ${}_eU_{21}$ and ${}_eU_{22}$ have two hyperbolic nodal-lines at $\eta = 1.207$ and $\eta = 1.319$, respectively and *2)* the odd modes ${}_oU_{21}$ and ${}_oU_{22}$ present two straight nodal-lines at x-axis and y-axis, respectively. Additionally the second modes ${}_{e,o}U_{22}(\xi,\eta,t)$ have two elliptic nodal-lines at $\xi = 0.257$ and $\xi = 0.374$, respectively.

5.5. Superposition of modes

As we mentioned in Sect. 4, the complete solution implies the superposition of even and odd modes. Let us consider this superposition for the second mode of the second harmonic (Fig. 9)

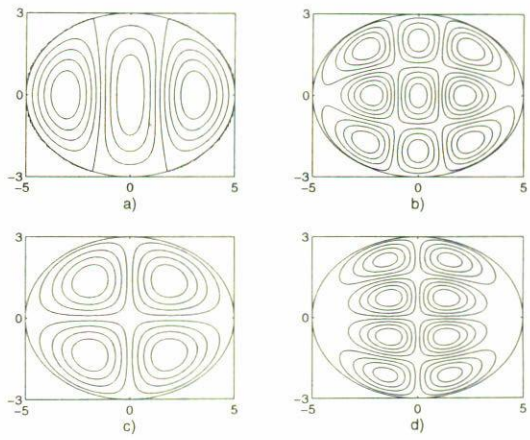

FIGURE 8. Contour plots of third harmonics a) ${}_eU_{21}(\xi,\eta)$; b) ${}_eU_{22}(\xi,\eta)$; c) ${}_oU_{21}(\xi,\eta)$; d) ${}_oU_{22}(\xi,\eta)$. We can appreciate that now the third harmonics present hyperbolic nodal lines as well.

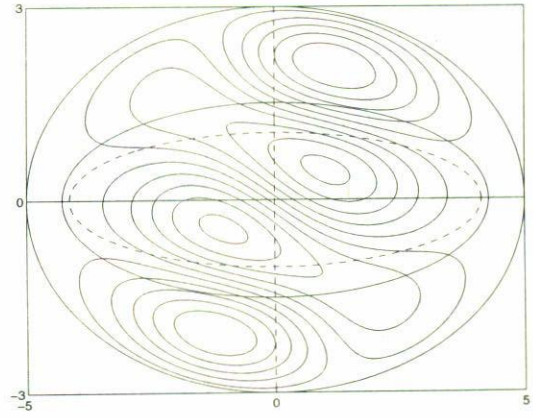

FIGURE 9. Contour plot of $U_{12} = {}_eU_{12} + {}_oU_{12}$ for an ellipse with $e = 0.8$. The dashed and continuous inner ellipses correspond to original nodal lines from ${}_eU_{12}$ and ${}_oU_{12}$.

$$U_{12}(\xi,\eta) =_e U_{12}(\xi,\eta) +_o U_{12}(\xi,\eta).$$

From Table III we can observe that ${}_o\omega_{12}/{}_e\omega_{12} = 1.154$, therefore ${}_oU_{12}$ oscillates 15.4% faster than ${}_eU_{11}$. Due to this difference in frequency, the shape of $U_{12}(\xi,\eta)$ is variable in time. On the contrary, let us suppose that we split the shape of the circular mode $U_{12}(\rho,\eta)$ into an even and an odd mode (symmetric and anti-symmetric with respect to $\eta = 0$, respectively). Due to the radial symmetry, both modes vibrate at the same frequency and the shape of the superposition-mode maintains constant in time, hence the separation is irrelevant. This is a very important difference between the circular membrane and elliptical membrane.

The dashed ellipse and dashed y-axis in Fig. 9 correspond to the original nodal-lines of ${}_eU_{12}$ (Fig. 7b). In the same manner, the continuous ellipse and continuous x-axis correspond to the original nodal-lines of ${}_oU_{12}$ (Fig. 7d). The cross-points

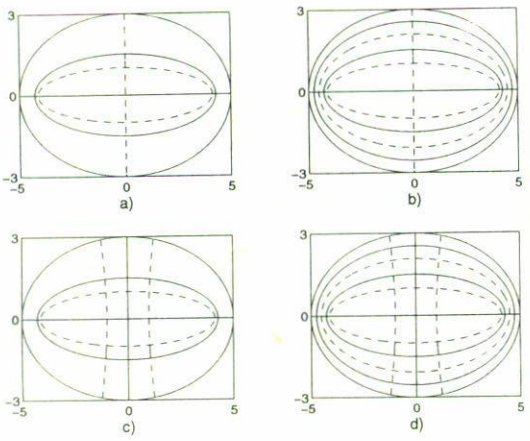

FIGURE 10. Superposition of nodal lines for several modes *a)* $U_{12}(\xi,\eta) = 5$ nodal-points; *b)* $U_{13}(\xi,\eta) = 9$ nodal-points; *c)* $U_{22}(\xi,\eta) = 10$ nodal-points; *d)* $U_{23}(\xi,\eta) = 18$ nodal-points. The cross-points between the dashed and continuous lines correspond to nodal-points.

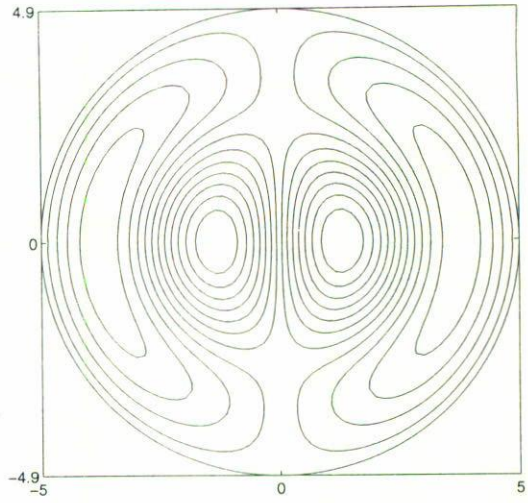

FIGURE 11. Contour plot of $U_{12} = {}_eU_{12} + {}_oU_{12}$ for an ellipse with $e = 0.2$. Observe the differences between this almost circular ellipse with respect to the ellipse with $e = 0.8$ in Fig. 9.

between the dashed lines and continuous lines correspond to *nodal-points* of the mode $U_{12}(\xi,\eta)$, in particular for this example we count 5 nodal-points.

In general, when we consider the superposition, the original nodal-lines of ${}_eU_{r,m}$ and ${}_oU_{r,m}$ become nodal-points of $U_{r,m}$.

By observation of the mode-patterns in Figs. 4, 7 and 8 we can conclude that the mode ${}_{e,o}U_{r,m}$ has

1. r angular nodal-lines corresponding to η = constant lines (*i.e.* straight or hyperbolic lines) and

2. m radial nodal-lines corresponding to ξ = constant lines (*i.e.* elliptic lines) including the boundary nodal-line.

In this manner, we can observe in Fig. 10a that by increasing m to 3, then appear two new elliptic nodal-lines corresponding to the even and odd mode respectively (Fig. 10b. These new nodal-lines generate four new nodal-points. On the other hand, if in Fig. 10a we increase r to 2, then appear two new hyperbolic nodal-lines (Fig. 10c) which generate five new nodal-points. Finally in Fig: 10d we show that mode U_{23} presents 18 nodal-points.

In order to generalize the before result, the number NP of nodal-points for a particular mode $U_{r,m}$ can be calculated with the following relation

$$NP = r + 4r(m-1) \qquad r \geq 1 \tag{54}$$

If $r = 0$ we have the fundamental harmonics which presents only even modes, therefore they have never nodal-points. Additionally, only the odd r-order modes present a nodal-point at origin.

Finally, we have chosen data from Table II to show in Fig. 11 the same mode $U_{12}(\xi,\eta)$ but now the eccentricity of the ellipse is given by $e = 0.2$. We can observe its notorious differences with respect to Fig. 9. On the other hand we can appreciate the similitudes between the pattern in Fig. 11 and the well-known circular mode-pattern [1, 3].

6. Conclusions

We have analyzed the solution of the wave equation in elliptic coordinates obtaining the characteristic frequencies and mode-equations in an elliptic membrane. The most important results for the elliptic membrane are summarized as follows.

- Except for the fundamental harmonics ($r = 0$), each mode $U_{r,m}$ in the elliptic membrane can be separated into an even mode ${}_eU_{r,m}$ and an odd mode ${}_oU_{r,m}$. The even mode is associated to major axis whereas the odd mode is associated to minor axis. This separation is irrelevant in a circular membrane.

- The even and odd modes of a particular mode $U_{r,m}$ vibrate with different frequencies, consequently, the shape of $U_{r,m}$ is not steady in time. In a circular membrane, this pattern is constant in time.

- The odd modes oscillate faster than even modes. The difference in frequency increases with eccentricity of ellipse. In this manner, if $e \to 0$, both frequencies get closer and tend to the frequency of the circular membrane.

- The nodal-lines in the circular membrane are straight diameters and concentric circles, while on the contrary, in the elliptical membrane the nodal-lines of ${}_eU_{r,m}$ and ${}_oU_{r,m}$ are straight axes and confocal hyperbolas and ellipses.

- The nodal-lines of ${}_eU_{r,m}$ are different to nodal-lines of ${}_oU_{r,m}$. Therefore, $U_{r,m}$ presents nodal-points corresponding to the cross-points between the nodal-lines of ${}_eU_{r,m}$ and ${}_oU_{r,m}$. The number of nodal-points in given by Eq. (54). The origin is a nodal-point of $U_{r,m}$ only if r is an odd number.

The oscillating modes can be expressed as a linear combination of Mathieu functions. We have shown graphically typical mode-patterns for different eccentricities of the elliptic boundary. The effect of ellipticity on the modal characteristic frequencies has been found to be of great importance on the mode structure. We have also presented interesting differences between the circular and elliptical membranes. We have introduced a formula to obtain the number of nodal points, in a particular the mode $U_{r,m}$. We expect that our results can be of great help in the studies of physical systems with elliptical geometry.

7. Appendix A. Computational considerations

In this Appendix we comment several remarks about the programming of Mathieu functions. We have used MATLAB software [8] to develop the routines.

In order to evaluate the Mathieu functions we apply the following procedure. First we calculate the characteristic values by solving the continued fractions (21)–(24). Several methods of evaluation of continued fractions exist [9, 9]. We follow the suggestion of Toyama and Shogen [11]. We truncate the continued fractions up to twelve elements and we develop algebraically the resulting expressions to obtain four polynomials of 12-degree. The roots of this polynomials are the characteristic values. Twelve elements of continued fractions were enough to assure the accuracy of more than 10^{-9}.

The Fourier coefficients for ce_r (or se_r) can be computed by using the particular characteristic value a_r (or b_r) and the recurrence relations (17a)–(20b). First we compute the coefficients A_k (or B_k) for $k = k_{\max}, k_{\max} - 2, \cdots, r$ by using backward recurrence. $k_{\max}$ is calculated for a tolerance tol by applying

$$|G_{2k+2}| = \left|\frac{A_{2k+2}}{A_{2k}}\right| = tol \sim \frac{q}{(2k_{\max}+2)^2}$$

The coefficients A_k (or B_k) for $k = 0, 2, \cdots, r$ (or $k = 1, 3, \cdots, r$) are determined by forward recurrence. The coefficient A_r calculated by using backward and forward recurrence must be equal, consequently we scale the coefficients computed by using backward recurrence to satisfy this condition. We rescale all coefficients to satisfy the normalization (31). Finally we compute the OMF by using Eqs. (26)–(29).

The MMF were calculated by applying Eqs. (55)–(58). The Bessel series for MMF are preferable for calculating the modified functions because they converge faster than hyperbolic series Eqs. (32)–(35).

$$Ce_{2n}(q,\xi) = \frac{ce_{2n}(q,0)}{A_0}\sum_{k=0}^{\infty} A_{2k}J_{2k}(u), \tag{55}$$

$$Ce_{2n+1}(q,\xi) = \frac{ce'_{2n+1}(q,\frac{\pi}{2})}{\sqrt{q}A_1} \times \sum_{k=0}^{\infty}(-1)^{k+1}A_{2k+1}J_{2k+1}(w), \tag{56}$$

$$Se_{2n+2}(q,\xi) = \frac{se'_{2n+2}(q,\frac{\pi}{2})}{qB_2}\tanh\xi \times \sum_{k=0}^{\infty}(-1)^{k+1}(2k+2)B_{2k+2}J_{2k+2}(w), \tag{57}$$

$$Se_{2n+1}(q,\xi) = \frac{se'_{2n+1}(q,0)}{\sqrt{q}B_1}\sum_{k=0}^{\infty} B_{2k+1}J_{2k+1}(u), \tag{58}$$

where

$$u = 2\sqrt{q}\sinh\xi \quad \text{and} \quad w = 2\sqrt{q}\cosh\xi.$$

To obtain the characteristic parameters ${}_{e,o}q_{r,m}$ for the membrane, we plot the MMF as function of q to estimate a coarse value (*i.e.* Fig. 2) . Later we use a MATLAB-algorithm to obtain the zeros. This algorithm uses a combination of bisection, secant, and inverse quadratic interpolation methods.

1. G.F. Simmons, *Ecuaciones Diferenciales*, segunda edición, (McGraw-Hill, México, 1993).
2. M. Boas, *Mathematical Methods in the Physical Sciences*, second edition, (Wiley, USA, 1983).
3. W. Kaplan, *Advanced Mathematics*, (Fondo Educativo Interamericano, México, 1985).
4. Emile Mathieu, *Jour. de Math. Pures et Appliquées* (Jour. de Liouville) **13** (1868) 137.
5. N.W. McLachlan, *Theory and application of Mathieu functions*, (Oxford Press, UK, 1951).
6. Lawrence Ruby, *Am. J. Phys.* **64** (1996) 39.
7. M. Abramowitz and I. Stegun, *Handbook of Mathematical functions*, (Dover, USA, 1965).
8. MatLab, Version 5.2, The Mathworks Inc., (1997).
9. G. Blanch, *SIAM Review* **6** (1964) 383.
10. W.H. Press, S.A. Teukolsky, W. Vetterling, and B. Flaneery, *Numerical Recipes*, second edition, (Cambridge Press, UK, 1997).
11. N. Toyama and K. Shogen, *IEEE Trans. Antennas & Prop* **AP-32** (1984) 537.